Identification of Fault Locations using Transient State Estimation

K. K.C. Yu, *Student Member, IEEE* and N. R. Watson, *Senior Member, IEEE*

Abstract—In a large scale electrical power system, identification of system faults can be a tedious task. Unexpected fault events, which affect all customers, must be identified quickly so appropriate action can be taken out. Due to the unknown changes in the system topology during fault condition, accurate fault assessment through EMTP/ATP is prohibited. Furthermore, exhaustive search performed through traditional methods is time consuming and requires good knowledge of the fault event prior to the search. In this paper, an alternative methodology in fault identification via Transient State Estimation (TSE) is presented. The TSE algorithm models the a.c. system in its equivalent circuit where a set of current and voltage state equations can be developed to form the measurement system. Estimation of the complete system state from limited measurements is achieved by solving the measurement system equations and hence the fault positions and its magnitude can be determined by looking at the nodal current mismatch in the system. Simulation results from the Lower South Island of the New Zealand system are used to validate this approach.

Keywords: Fault identification, State estimation, Electromagnetic transients

I. INTRODUCTION

WHEN a fault has occurred in a large power system, it is usually a difficult task to determine the fault position. Regardless of whether it occurred at transmission or load level, all customers that are connected to it will be affected to some degree. It is important the fault position is quickly identified so appropriate action can be carried out. Due to the measurement cost, complete monitoring of the system to determine the fault event is impractical. Therefore, when a transient event is recorded, the fault information available is often very limited. One method is to simulate the possible fault events through computer simulation EMTP/ATP [1]-[2] and then compares the simulation results with the actual recorded transient response. A good indication of the fault is achieved if the transient responses are closely matched. This exhaustive search method is arbitrary; the fact that it needs to simulate the possible fault events and compares with the actual response is time consuming and requires a good knowledge of all the possible

fault events prior to the search. In this paper, a new fault identification methodology via transient state estimation technique is presented. The proposed method estimates the complete system state and power flow from partial measurements at each time-step. Once the complete system state is known, the fault position can be determined from the power flow accordingly.

An electrical power system expanded in its discrete equivalent RLC branches can be described by a set of current and voltage state equations. By combining these equations with appropriate state variables, the complete state model of the power system is achieved. The set of system equations can be formed without knowing the set of independent state variables, but are bounded by topological constraints (i.e. interconnection) and algebraic constraints. This is beneficial particularly in large power systems where independency of the state variables is not obviously apparent due to the presence of network intervening.

Complete estimation of the system state requires the system to be fully observable. The system is said to be fully observable if the measurement system solves the state variables uniquely. By converting the system differential equations to discrete time equations using Euler's rule, history values at previous time-step can be used as additional measurements when forming the measurement system. These additional measurements act as measurement noise filter in over-determined system or provide extra measurement information in under-determined system.

The test system used to validate the proposed method is taken from the Lower South Island of the New Zealand.

II. FORMULATION OF THE STATE EQUATIONS

Power system modelled by its lumped RLC equivalents can be described as a set of first order differential equations. These equations describe the interconnection between the RLC branches and the state variables. The relevant system components are modelled as follows:

1. Generators: these are modelled by a voltage source with their equivalent R-R//L impedance.
2. Transformers: they are represented using two windings model depending on the type of magnetic circuit and on the connections of the terminals and the neutrals. i.e. delta or wye. Core losses are represented internally with an equivalent shunt resistance across each winding in the transformer.
3. Transmission lines: these are modelled by the three-phase

PI models and hence capable of incorporating non symmetric condition.
4. Loads: The real and reactive power components are represented by its equivalent resistance and inductance respectively.

A   Transformer Model

A two windings transformer model is used in the TSE algorithm. It is capable of modelling different impedance to the different components of current depending on the type of magnetic circuit and on the connections of the terminals & the neutral. Fig. 1 shows the two windings Y-G/Y-G connected transformer model. It is possible to simplify the three-phase transformers model by ignoring the interphase mutuals and reducing the equations to three independent sets of the three phases. This is accurate when banks of single-phase units are used. Effects like phase shifts, zero sequence circulating currents, etc are catered for by the terminal connections. Off-nominal taps on either primary or secondary winding can be represented by scaling the self and mutual elements accordingly.
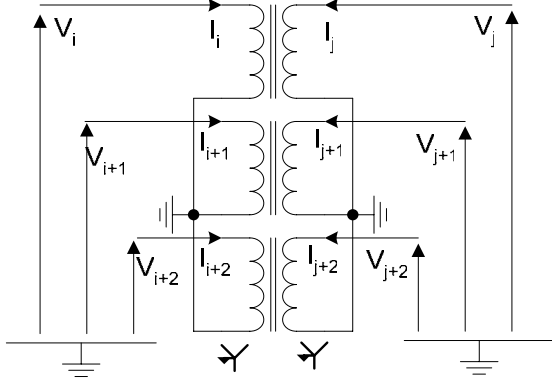

Fig. 1. Three phase Y-G/Y-G connected transformer

Neglecting core losses, the differential equations for a three phase transformer can be expressed as:

$$\frac{d}{dt}\begin{bmatrix} I_i \\ I_{i+1} \\ I_{i+2} \\ I_j \\ I_{j+1} \\ I_{j+2} \end{bmatrix} = \left[K_{i_{nb}}\right]^{-1}\begin{bmatrix} L_{i,i} & L_{i,j} & 0 & 0 & 0 & 0 \\ L_{j,i} & L_{j,j} & 0 & 0 & 0 & 0 \\ 0 & 0 & L_{i+1,i+1} & L_{i+1,j+1} & 0 & 0 \\ 0 & 0 & L_{j+1,i+1} & L_{j+1,j+1} & 0 & 0 \\ 0 & 0 & 0 & 0 & L_{i+2,i+2} & L_{i+2,j+2} \\ 0 & 0 & 0 & 0 & L_{j+2,i+2} & L_{j+2,j+2} \end{bmatrix}^{-1}\left[K_{v_{nb}}\right]\begin{bmatrix} V_i \\ V_{i+2} \\ V_{i+2} \\ V_j \\ V_{j+1} \\ V_{j+2} \end{bmatrix} \quad (1)$$

for Y-G/Y-G configuration, $\left[K_{i_{nb}}\right] = \left[K_{v_{nb}}\right] = \begin{bmatrix} 1 & 0 & 0 & 0 & 0 & 0 \\ 0 & 1 & 0 & 0 & 0 & 0 \\ 0 & 0 & 1 & 0 & 0 & 0 \\ 0 & 0 & 0 & 1 & 0 & 0 \\ 0 & 0 & 0 & 0 & 1 & 0 \\ 0 & 0 & 0 & 0 & 0 & 1 \end{bmatrix}$

where

$K_{v_{nb}}$ and $K_{i_{nb}}$ are the branch-node incidence (connection) for voltages and currents respectively.

L_{ii} is the self inductance.

L_{ij}, L_{ji} are the mutual inductance.

B   Transmission Line Model

A three phase PI model is used to represent short to medium length transmission line in the TSE algorithm. The model includes transmission line coupling effects. Fig. 2 shows the transmission line PI model.

Kirchhoff's laws are used to form the algebraic equations as shown in (2). These equations are used to derive the transmission line model expressed in (3).

$$I_s = I_L + \frac{I_{sh}}{2}$$

$$I_r = I_L - \frac{I_{sh}}{2} \quad (2)$$

$$V_s = [R_s]I_L + [L_s]\frac{dI_L}{dt} + V_r$$

$$\frac{d}{dt}\begin{bmatrix} I_L \\ L \\ V_s \\ L \\ V_r \end{bmatrix} = \begin{bmatrix} 0 & -[L_s]^{-1}[R_s] & 0 & [L_s]^{-1} & -[L_s]^{-1} \\ L & L & L & L & L \\ \left[\frac{C_{sh}}{2}\right]^{-1} & -\left[\frac{C_{sh}}{2}\right]^{-1} & 0 & -\left[\frac{C_{sh}}{2}\right]^{-1}\left[\frac{2}{R_{sh}}\right] & 0 \\ L & L & L & L & L \\ 0 & \left[\frac{C_{sh}}{2}\right]^{-1} & -\left[\frac{C_{sh}}{3}\right]^{-1} & 0 & -\left[\frac{C_{sh}}{2}\right]^{-1}\left[\frac{2}{R_{sh}}\right] \end{bmatrix}\begin{bmatrix} I_s \\ I_L \\ I_r \\ V_s \\ V_r \end{bmatrix} \quad (3)$$

where

I_s, I_r, I_L, I_{sh} are sending end currents, receiving end currents, inductor currents and shunt currents

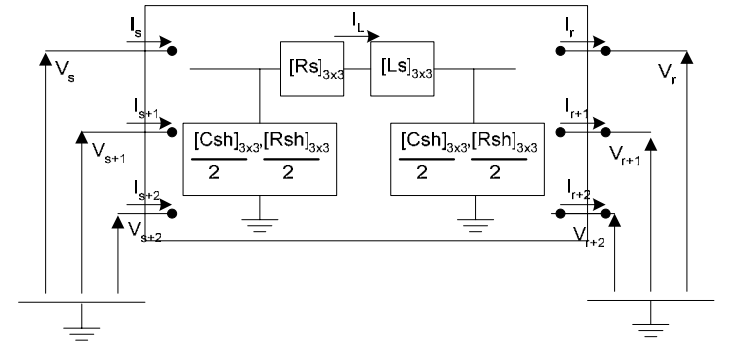V_s, V_r are sending and receiving end voltages.

Fig. 2. Three phase transmission line PI model

C   Load Model

The algorithm models the system load by its equivalent resistance and reactance as shown in Fig. 3. Its state equations are described in (4).
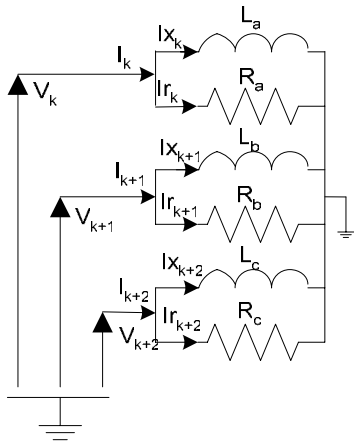
Fig. 3. Three phase load model

$$
\begin{bmatrix}
\dfrac{d}{dt}(Ix_k) \\
\dfrac{d}{dt}(Ix_{k+1}) \\
\dfrac{d}{dt}(Ix_{k+2}) \\
I_k \\
I_{k+1} \\
I_{k+2}
\end{bmatrix}
=
\begin{bmatrix}
0 & 0 & 0 & L_a^{-1} & 0 & 0 \\
0 & 0 & 0 & 0 & L_b^{-1} & 0 \\
0 & 0 & 0 & 0 & 0 & L_c^{-1} \\
1 & 0 & 0 & R_a^{-1} & 0 & 0 \\
0 & 1 & 0 & 0 & R_b^{-1} & 0 \\
0 & 0 & 1 & 0 & 0 & R_c^{-1}
\end{bmatrix}
\begin{bmatrix}
Ix_k \\
Ix_{k+1} \\
Ix_{k+2} \\
V_k \\
V_{k+1} \\
V_{k+2}
\end{bmatrix}
\quad (4)
$$

III. DIFFERENCE EQUATIONS

TSE is performed recursively for each time-step, hence discretisation of the continuous time differential equations is necessary. The operator d/dt can be approximated using Euler's formula as shown in (5). Equations (1), (3) and (4) can then be expressed as in (6), (7) and (8) respectively.

$$
y_{t+\Delta t} = y_t + \Delta t f_{t+\Delta t} \quad (5)
$$

$$
\begin{bmatrix}
I_i \\
I_{i+1} \\
I_{i+1} \\
I_j \\
I_{j+1} \\
I_{j+2}
\end{bmatrix}_{t-\Delta t}
=
\begin{bmatrix}
I_i \\
I_{i+1} \\
I_{i+2} \\
I_j \\
I_{j+1} \\
I_{j+2}
\end{bmatrix}_t
- \Delta t \left(\left[K_{i_{nb}}\right]^{-1} \left[L\right]^{-1} \left[K_{v_{nb}}\right] \right)
\begin{bmatrix}
V_i \\
V_{i+1} \\
V_{i+2} \\
V_j \\
V_{j+1} \\
V_{j+2}
\end{bmatrix}_t
$$

$$
where \quad [L] =
\begin{bmatrix}
L_{i,i} & L_{i,j} & 0 & 0 & 0 & 0 \\
L_{j,i} & L_{j,j} & 0 & 0 & 0 & 0 \\
0 & 0 & L_{i+1,i+1} & L_{i+1,j+1} & 0 & 0 \\
0 & 0 & L_{j+1,i+1} & L_{j+1,j+1} & 0 & 0 \\
0 & 0 & 0 & 0 & L_{i+2,i+2} & L_{i+2,j+2} \\
0 & 0 & 0 & 0 & L_{j+2,i+2} & L_{j+2,j+2}
\end{bmatrix}
\quad (6)
$$

$$
\begin{bmatrix}
\dfrac{I_L}{L} \\
\dfrac{V_s}{L} \\
V_r
\end{bmatrix}_{t-\Delta t}
= \Delta t [M]
\begin{bmatrix}
I_s \\
I_L \\
I_r \\
V_s \\
V_r
\end{bmatrix}_t
\quad (7)
$$

where

$$
[M] =
\begin{bmatrix}
0 & \dfrac{[L_s]^{-1}[R_s]}{L} & 0 & \dfrac{-[L_s]^{-1}}{L} & \dfrac{[L_s]^{-1}}{L} \\
-\dfrac{\left[\frac{C_{sh}}{2}\right]^{-1}}{L} & \dfrac{\left[\frac{C_{sh}}{2}\right]^{-1}}{L} & 0 & \dfrac{\left[\frac{C_{sh}}{2}\right]^{-1}\left[\frac{2}{R_{sh}}\right]+[1]}{L} & 0 \\
0 & -\dfrac{\left[\frac{C_{sh}}{2}\right]^{-1}\left[\frac{C_{sh}}{3}\right]^{-1}}{L} & 0 & 0 & \left[\frac{C_{sh}}{2}\right]^{-1}\left[\frac{2}{R_{sh}}\right]+[1]
\end{bmatrix}
$$

$$
\begin{bmatrix}
Ix_k \big|_{t-\Delta t} \\
Ix_{k+1} \big|_{t-\Delta t} \\
Ix_{k+2} \big|_{t-\Delta t} \\
I_k \big|_t \\
I_{k+1} \big|_t \\
I_{k+2} \big|_t
\end{bmatrix}
=
\begin{bmatrix}
1 & 0 & 0 & \Delta t L_a^{-1} & 0 & 0 \\
0 & 1 & 0 & 0 & \Delta t L_b^{-1} & 0 \\
0 & 0 & 1 & 0 & 0 & \Delta t L_c^{-1} \\
1 & 0 & 0 & R_a^{-1} & 0 & 0 \\
0 & 1 & 0 & 0 & R_b^{-1} & 0 \\
0 & 0 & 1 & 0 & 0 & R_c^{-1}
\end{bmatrix}
\begin{bmatrix}
Ix_k \\
Ix_{k+1} \\
Ix_{k+2} \\
V_k \\
V_{k+1} \\
V_{k+2}
\end{bmatrix}_t
\quad (8)
$$

The discretised state equations in terms of state variables at previous time step are advantageous in forming the measurement system. It allows history values ($t-\Delta t$) to be used as virtual measurements (i.e. measurements do not need metering) as well as real-time measurements.

By inspecting (7), it is shown that the transmission line inductor current can be used as measurements when forming the measurement system, however, given that it is usually not a well defined variable (i.e. difficult to measure) in a practical system, the sending end and receiving branch currents are used instead. The state equations become:

$$
\begin{bmatrix}
I_s \\
I_{s+1} \\
I_{s+2}
\end{bmatrix}_t'
=
\begin{bmatrix}
1 & 0 & 0 & \dfrac{C_{sh_{s,s}}}{2\Delta t}+\dfrac{2}{R_{sh_{s,s}}} & \dfrac{C_{sh_{s,s+1}}}{2\Delta t}+\dfrac{2}{R_{sh_{s,s+1}}} & \dfrac{C_{sh_{s,s+2}}}{2\Delta t}+\dfrac{2}{R_{sh_{s,s+2}}} \\
0 & 1 & 0 & \dfrac{C_{sh_{s+1,s}}}{2\Delta t}+\dfrac{2}{R_{sh_{s+1,s}}} & \dfrac{C_{sh_{s+1,s+1}}}{2\Delta t}+\dfrac{2}{R_{sh_{s+1,s+1}}} & \dfrac{C_{sh_{s+1,s+2}}}{2\Delta t}+\dfrac{2}{R_{sh_{s+1,s+2}}} \\
0 & 0 & 1 & \dfrac{C_{sh_{s+2,s}}}{2\Delta t}+\dfrac{2}{R_{sh_{s+2,s}}} & \dfrac{C_{sh_{s+2,s+1}}}{2\Delta t}+\dfrac{2}{R_{sh_{s+2,s+1}}} & \dfrac{C_{sh_{s+2,s+2}}}{2\Delta t}+\dfrac{2}{R_{sh_{s+2,s+2}}}
\end{bmatrix}
\begin{bmatrix}
I_L \\
I_{L+1} \\
I_{L+2} \\
V_s \\
V_{s+1} \\
V_{s+2}
\end{bmatrix}_t
$$

where

$$
\begin{bmatrix}
I_s \\
I_{s+1} \\
I_{s+2}
\end{bmatrix}_t'
=
\begin{bmatrix}
I_s \\
I_{s+1} \\
I_{s+2}
\end{bmatrix}_t
+
\begin{bmatrix}
\dfrac{C_{sh_{s,s}}}{2\Delta t} & \dfrac{C_{sh_{s,s+1}}}{2\Delta t} & \dfrac{C_{sh_{s,s+2}}}{2\Delta t} \\
\dfrac{C_{sh_{s+1,s}}}{2\Delta t} & \dfrac{C_{sh_{s+1,s+1}}}{2\Delta t} & \dfrac{C_{sh_{s+1,s+2}}}{2\Delta t} \\
\dfrac{C_{sh_{s+2,s}}}{2\Delta t} & \dfrac{C_{sh_{s+2,s+1}}}{2\Delta t} & \dfrac{C_{sh_{s+2,s+2}}}{2\Delta t}
\end{bmatrix}
\begin{bmatrix}
V_s \\
V_{s+1} \\
V_{s+2}
\end{bmatrix}_{t-\Delta t}
\quad (9)
$$

$$\begin{bmatrix} I_r \\ I_{r+1} \\ I_{r+2} \end{bmatrix}'_t = \begin{bmatrix} 1 & 0 & 0 & \dfrac{-C_{sh_{s,s}}}{2\Delta t} - \dfrac{2}{R_{sh_{s,s}}} & \dfrac{-C_{sh_{s,s+1}}}{2\Delta t} - \dfrac{2}{R_{sh_{s,s+1}}} & \dfrac{-C_{sh_{s,s+2}}}{2\Delta t} - \dfrac{2}{R_{sh_{s,s+2}}} \\ 0 & 1 & 0 & \dfrac{-C_{sh_{s+1,s}}}{2\Delta t} - \dfrac{2}{R_{sh_{s+1,s}}} & \dfrac{-C_{sh_{s+1,s+1}}}{2\Delta t} - \dfrac{2}{R_{sh_{s+1,s+1}}} & \dfrac{C_{sh_{s+1,s+2}}}{2\Delta t} - \dfrac{2}{R_{sh_{s+1,s+2}}} \\ 0 & 0 & 1 & \dfrac{-C_{sh_{s+2,s}}}{2\Delta t} - \dfrac{2}{R_{sh_{s+2,s}}} & \dfrac{-C_{sh_{s+2,s+1}}}{2\Delta t} - \dfrac{2}{R_{sh_{s+2,s+1}}} & \dfrac{-C_{sh_{s+2,s+2}}}{2\Delta t} - \dfrac{2}{R_{sh_{s+2,s+2}}} \end{bmatrix} \begin{bmatrix} I_L \\ I_{L+1} \\ I_{L+2} \\ V_r \\ V_{r+1} \\ V_{r+2} \end{bmatrix}_t$$

where

$$\begin{bmatrix} I_r \\ I_{r+1} \\ I_{r+2} \end{bmatrix}'_t = \begin{bmatrix} I_r \\ I_{r+1} \\ I_{r+2} \end{bmatrix}_t - \begin{bmatrix} \dfrac{C_{sh_{s,s}}}{2\Delta t} & \dfrac{C_{sh_{s,s+1}}}{2\Delta t} & \dfrac{C_{sh_{s,s+2}}}{2\Delta t} \\ \dfrac{C_{sh_{s+1,s}}}{2\Delta t} & \dfrac{C_{sh_{s+1,s+1}}}{2\Delta t} & \dfrac{C_{sh_{s+1,s+2}}}{2\Delta t} \\ \dfrac{C_{sh_{s+2,s}}}{2\Delta t} & \dfrac{C_{sh_{s+2,s+1}}}{2\Delta t} & \dfrac{C_{sh_{s+2,s+2}}}{2\Delta t} \end{bmatrix} \begin{bmatrix} V_r \\ V_{r+1} \\ V_{r+2} \end{bmatrix}_{t-\Delta t} \qquad (10)$$

IV. TRANSIENT STATE ESTIMATION

The main purpose of TSE is to estimate the power flow of the whole network from limited synchronized measurements. Ideally, an accurate TSE requires:

1. Accurate modelling of the system topology.
2. The system to be fully observable for the given set of measurements (i.e. over-determined system).
3. Absence of bad measurements.

Consider a general measurement system which relates the measurement vector $\underline{z}$ to the state variables $\underline{x}$ expressed in (11)

$$\underline{z} = [H]\underline{x} + \underline{\varepsilon} \qquad (11)$$

where $\underline{\varepsilon}$ is the error vector and $[H]$ is the measurement matrix.

To build up the measurement system, rows are picked from the differential equations (6)-(10) for the corresponding measurements. In the case where field measurements data are absent, measurement data obtained from simulation can be used to supply to the TSE algorithm and are considers as the true measurements of the system states. The state variables to be estimated are the inductor currents and nodal voltages. Once they are obtained, the power flow of the whole network can be calculated accordingly. The procedure of the TSE can be described as follows:

1. Establish appropriate state model for linear and non linear system components, such as transformers and transmission lines.
2. Equate complete differential and algebraical equations for the power system. Euler's formula is used to discretise these equations in this case.
3. Read off-line (history) and on-line measurements from selected measurement locations.
4. Build up the measurements equations by adding rows of dynamics equations which relate the measurements to the state variables.

$$\underline{z} = [H]\underline{x} + \underline{\varepsilon}$$

5. Solve the measurement system for current time-step.

$$\underline{x} = \left([H]^T [H] \right)^{-1} [H]^T \underline{z}$$

6. Calculate dependent variables such as branch currents.
7. Record estimation and use as offline measurements ($\underline{z}_{t-\Delta t}$) for the next time-step.
8. Repeat 2-7 for the next time-step.

V. TEST SYSTEM AND SIMULATION RESULTS

The test system chosen is the Lower South Island of the New Zealand system. The system consists of 27 nodes and 87 branches. Three linear loads are located at Tiwai 220kV, Invercargill 33kV and Roxburgh 11kV. The symmetric and asymmetric measurement placements are shown in Fig. 4. Due to the lack of field measurements, the measurement data used are obtained from the Transient Converter Simulation (TCS) [3] based simulation. TCS is a nodal approach with diakoptical segregation of the plant components, specially developed to analyse the dynamic behavior of HVDC systems. method developed A 2.5 cycle duration symmetrical line-to-ground fault is simulated in the test system. The fault location is shown by the black crosses (doubt cct. transmission line) in Fig. 4.

Figs. 5-9 show the estimated voltages at Tiwai 220kV and receiving end line currents at Manapouri-Tiwai 220kV transmission line. The actual and estimated values are shown as dotted and solid line respectively. The difference is shown at the bottom half of the figure. Despite the difference occurred during the fault transition period (switched in/out), which is caused by an increase error in the Euler's approximation for very fast transients, the results show TSE is capable of estimating the network's behavior from the partial measurements.
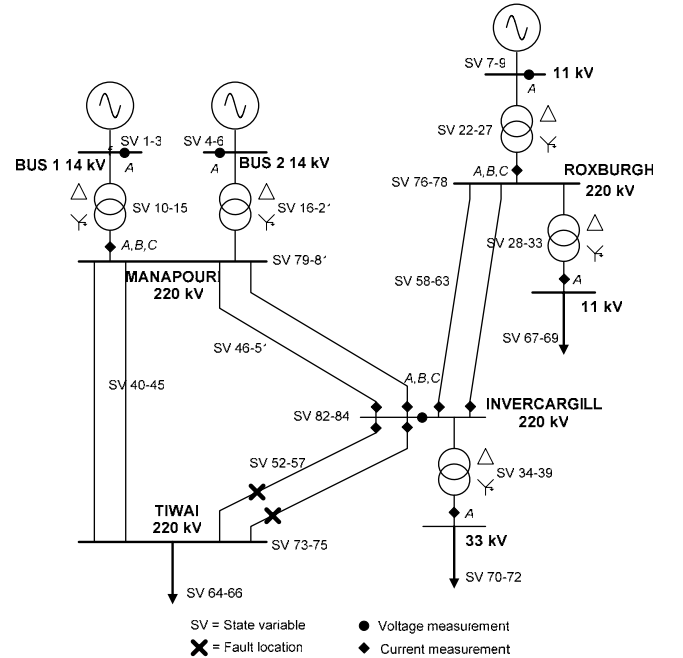

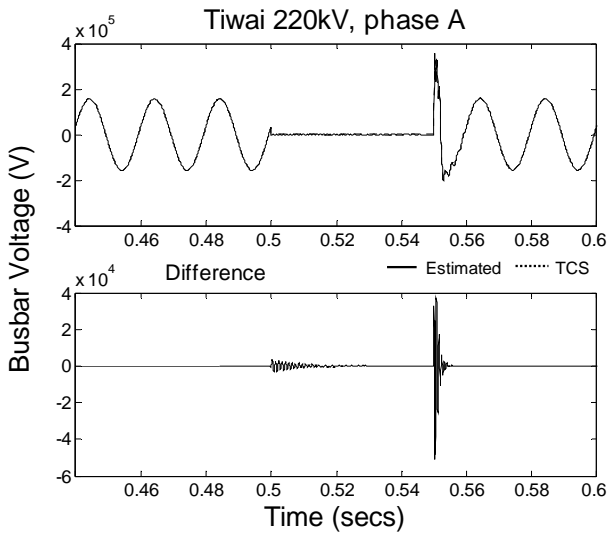Fig. 4. Lower South Island of the New Zealand System

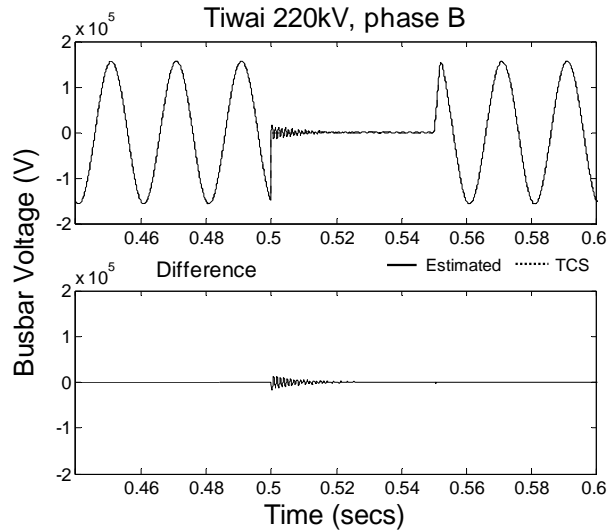Fig. 5. Busbar voltage at Tiwai 220kV, phase A

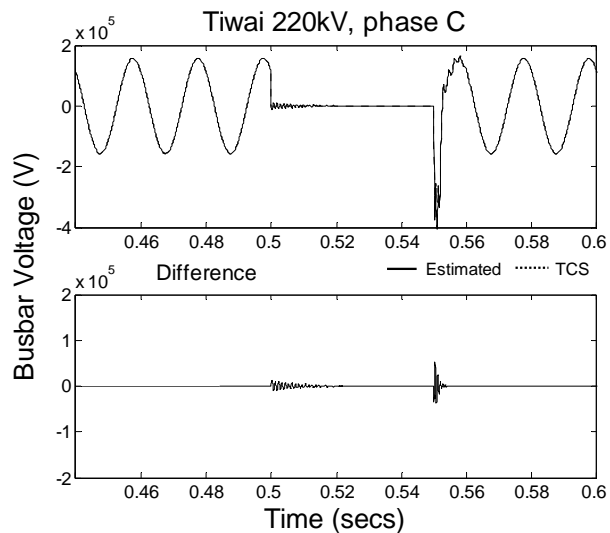Fig. 6. Busbar voltage at Tiwai 220kV, phase B

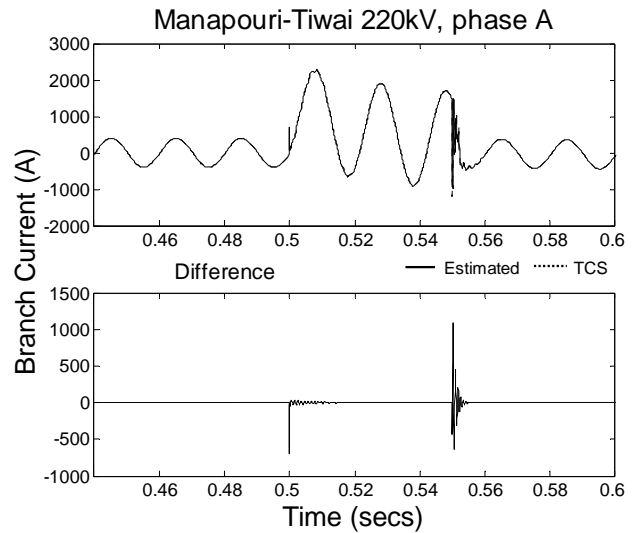Fig. 7. Busbar voltage at Tiwai 220kV, phase C

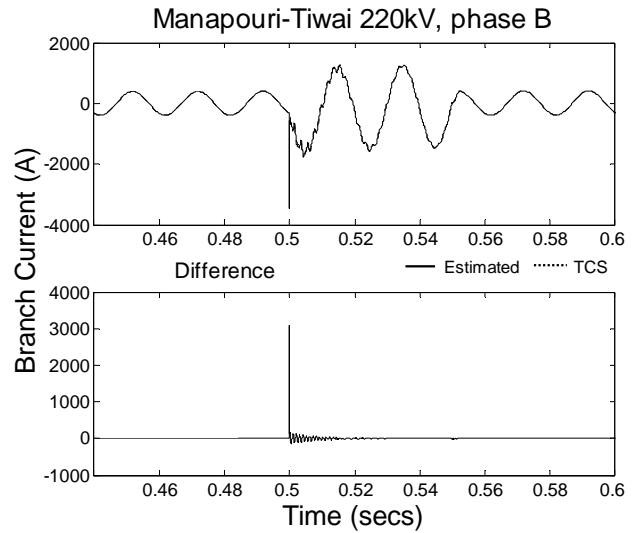Fig. 8. Branch current at Man-Tiw 220kV, phase A, receiving end

Fig. 9. Branch current at Man-Tiw 220kV, phase B, receiving end

To represent the unexpected fault event in the test system, the system topology supplied to the TSE during the fault period remained unchanged i.e. the fault is not modelled in the TSE. This causes inconsistent estimation results and hence current mismatch at the fault location during the fault period. Fig. 10 shows the nodal current mismatch of the test system. As indicated by the significant current mismatch positioned at nodes 1-3 (Tiwai 220kV), the followings are deduced:

1. The fault position is located at Tiwai 220kV (nodes 1-3)
2. The current mismatch at the Tiwai 220kV nodes represents the fault currents. Figs. 11-13 show the comparison of the current mismatch with the simulated fault current at each phase.
3. The fault is symmetrical as the fault currents are balanced.
4. Low fault resistance (estimated by the nodal voltage/fault current) suggests the type of fault is a line-to-ground fault.
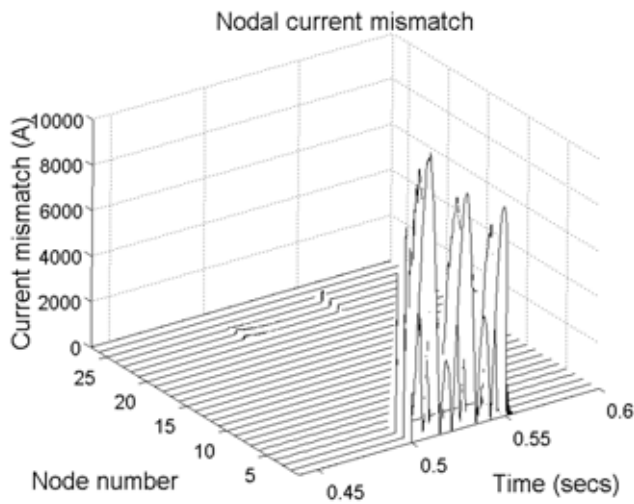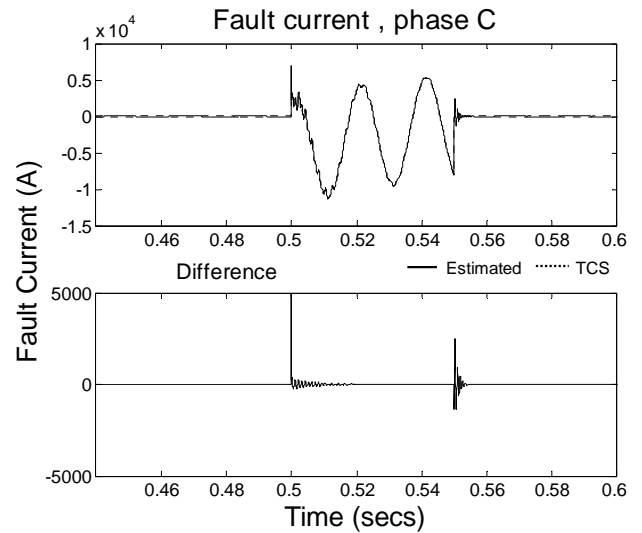
Fig. 10 Nodal current mismatch (absolute values)

Fig. 11. Fault current at phase A
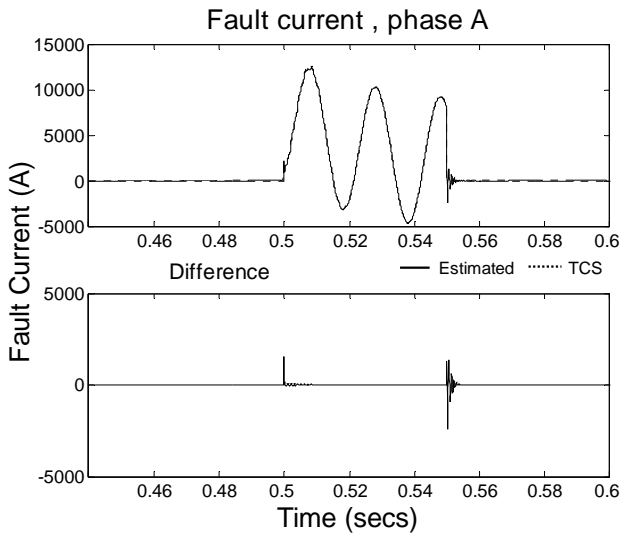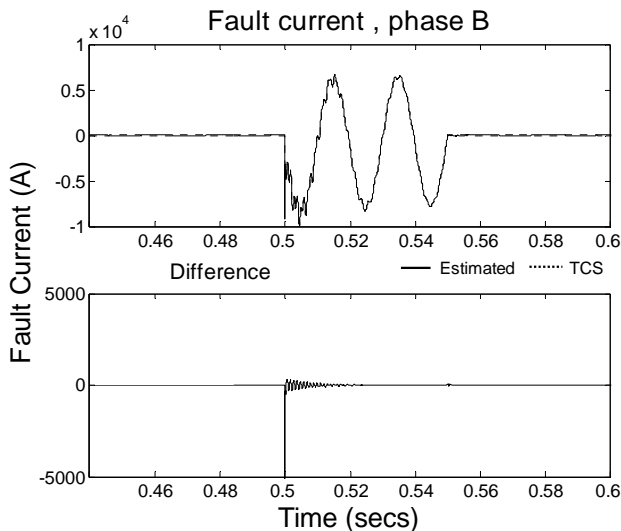

Fig. 12. Fault current at phase B

Fig. 13. Fault current at phase C

VI. CONCLUSION

At present, when a fault has occurred, the fault information available to identify its position is usually insufficient. In this paper, the use of TSE for fault identification, by estimating the complete system states from partial measurements, is presented. The discrete time state-space formulation allows historical system states to be used as measurements to provide additional measurement information. However, the time-step must be adequate to cater for fast transients when the operator d/dt is approximated using Euler's formula.

From the test results, the TSE solution showed agreement with the TCS based simulation. Three important fault characteristics: 1) the fault position, 2) fault type and 3) the magnitude of the fault currents, are obtained by inspecting the nodal current mismatch of the system. Fault identification via TSE technique is accurate, efficient and easy to implement.

VII. REFERENCES

[1] W. Long, D. Cotcher, D. Ruiu, P. Adam, S. Lee and R. Adapa, "EMTP-a powerful tool for analyzing power system transients," *IEEE Computer Application in Power*, vol. 3, no. 3, pp. 36-41, 1990

[2] J. J. Marti and L. R. Linares, "Real-Time EMTP- based transients simulation," *IEEE Trans. Power Systems,* vol. 9, no. 3, pp. 1309-1317, 1994

[3] J. Arrillaga, C. P. Arnold and B. J. Harker, "Computer modeling of electrical power system," J.Wiley & Sons, London, 1983

VIII. BIOGRAPHIES

Kent Yu completed his B.E. (Hons) in 2001 and is at present a Ph.D. candidate. His area of research is state estimation techniques.

Neville Watson received his B.E. (Hons) and Ph.D. degrees in electrical and electronic engineering from the University of Canterbury (New Zealand) where he is now a Senior Lecturer. His interests include power quality, steady-state and dynamic analysis of ac/dc power systems.